Extreme Suppression of Antiferromagnetic Order and Critical Scaling in a Two-Dimensional Random Quantum Magnet

Wenshan Hong, Lu Liu, Chang Liu, Xiaoyan Ma, Akihiro Koda, Xin Li, Jianming Song, Wenyun Yang, Jinbo Yang, Peng Cheng, Hongxia Zhang, Wei Bao, Xiaobai Ma, Dongfeng Chen, Kai Sun, Wenan Guo, Huiqian Luo, Anders W. Sandvik, and Shiliang Li

Phys. Rev. Lett. **126**, 037201 — Published 19 January 2021

DOI: 10.1103/PhysRevLett.126.037201

Extreme Suppression of Antiferromagnetic Order and Critical Scaling in a Two-Dimensional Random Quantum Magnet

Wenshan Hong,[1,2] Lu Liu,[1] Chang Liu,[1,2] Xiaoyan Ma,[1,2] Akihiro Koda,[3,4] Xin Li,[5] Jianming Song,[5] Wenyun Yang,[6] Jinbo Yang,[6] Peng Cheng,[7] Hongxia Zhang,[7] Wei Bao,[7,8] Xiaobai Ma,[9] Dongfeng Chen,[9] Kai Sun,[9] Wenan Guo,[10,11] Huiqian Luo,[1,12] Anders W. Sandvik,[13,1,*] and Shiliang Li[1,2,12,†]

[1]*Beijing National Laboratory for Condensed Matter Physics, Institute of Physics, Chinese Academy of Sciences, Beijing 100190, China*
[2]*School of Physical Sciences, University of Chinese Academy of Sciences, Beijing 100190, China*
[3]*Institute of Materials Structure Science, High Energy Accelerator Research Organization (KEK-IMSS),1-1 Oho, Tsukuba 305-0801, Japan*
[4]*Department of Materials Structure Science, Sokendai (The Graduate University for Advanced Studies), Tsukuba, Ibaraki, 305-0801, Japan*
[5]*Key Laboratory of Neutron Physics and Institute of Nuclear Physics and Chemistry, China Academy of Engineering Physics, Mianyang 621999, China*
[6]*State Key Laboratory for Mesoscopic Physics, School of Physics, Peking University, Beijing, 100871, China*
[7]*Department of Physics and Beijing Key Laboratory of Opto-electronic Functional Materials & Micro-nano Devices, Renmin University of China, Beijing 1 00872, China*
[8]*Department of Physics, City Univesity of Hong Kong, Kowloon, Hong Kong*
[9]*Department of Nuclear Physics, China Institute of Atomic Energy, Beijing, 102413, China*
[10]*Department of Physics, Beijing Normal University, Beijing 100875, China*
[11]*Beijing Computational Science Research Center, Beijing 100193, China*
[12]*Songshan Lake Materials Laboratory, Dongguan, Guangdong 523808, China*
[13]*Department of Physics, Boston University, 590 Commonwealth Avenue, Boston, Massachusetts 02215, USA*

(Dated: July 24, 2020)

Sr_2CuTeO_6 is a square-lattice Néel antiferromagnet with superexchange between first-neighbor $S = 1/2$ Cu spins mediated by plaquette centered Te ions. Substituting Te by W, the affected impurity plaquettes have predominantly second-neighbor interactions, thus causing local magnetic frustration. Here we report a study of $Sr_2CuTe_{1-x}W_xO_6$ using neutron diffraction and μSR techniques, showing that the Néel order vanishes already at $x = 0.025 \pm 0.005$. We explain this extreme order suppression using a two-dimensional Heisenberg spin model, demonstrating that a W-type impurity induces a deformation of the order parameter that decays with distance as $1/r^2$ at temperature $T = 0$. The associated logarithmic singularity leads to loss of order for any $x > 0$. Order for small $x > 0$ and $T > 0$ is induced by weak interplane couplings. In the nonmagnetic phase of $Sr_2CuTe_{1-x}W_xO_6$, the μSR relaxation rate exhibits quantum critical scaling with a large dynamic exponent, $z \approx 3$, consistent with a random-singlet state.

A central theme in modern condensed matter physics is the evolution of two-dimensional (2D) quantum antiferromagnets upon doping, as epithomized by the high-T_c cuprates with charge carriers introduced into the CuO_2 layers through off-layer doping [1, 2]. In-plane static impurities have also been studied, e.g., non-magnetic Zn substituting the spin $S = 1/2$ carrying Cu ions [3–5]. In general, impurities and random frustrated couplings in a quantum magnet will eventually destroy any order and may induce not yet fully understood disordered states, e.g., quantum spin glasses [6–8], spin fluids [9], valence-bond glasses [10, 11], and random-singlet (RS) states [12–24].

We here report μSR and neutron diffraction experiments on $Sr_2CuTe_{1-x}W_xO_6$, which at $x = 0$ realizes the 2D $S = 1/2$ antiferromagnetic (AFM) Heisenberg model with predominantly first-neighbor interactions J_1 generated through superexchange via Te ions at the centers of the plaquettes of 2×2 Cu ions [25, 26]; see Fig. 1(a). At $x = 1$, the W ions instead mediate second-neighbor superexchange in the affected plaquettes, Fig. 1(b), with $J_2 \approx J_1$ [27–29]. An intriguing magnetically disordered state exists within a window $[x_{c1}, x_{c2}]$, with $x_{c1} \approx 0.1$ and $x_{c2} \approx 0.6$ estimated [30–32]. The ability to tune the disorder and frustration by x offers unique opportunities to systematically study frustrated plaquette impurities of the J_2 type illustrated in Fig. 1(c) for small x and the subsequent randomness-induced non-magnetic state for larger x.

We demonstrate destruction of the Néel order in $Sr_2CuTe_{1-x}W_xO_6$ at $x_{c1} = 0.025 \pm 0.005$, far below the previous estimate. We explain this dramatic order suppression using a classical Heisenberg model with random W and Te

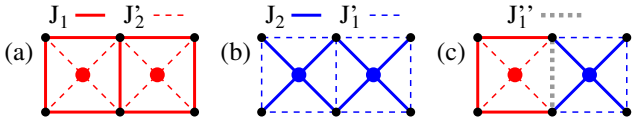

Figure 1. 2D Heisenberg couplings $J_{ij}\mathbf{S}_i \cdot \mathbf{S}_j$ in $Sr_2CuTe_{1-x}W_xO_6$. The small black circles represent the $S = 1/2$ carrying Cu ions, while red and blue circles correspond to Te and W ions, respectively. The dominant couplings mediated by Te in (a) and W in (b) are first-neighbor J_1 (solid red lines) and second-neighbor J_2 (solid blue lines), with $J_1 \approx J_2 \approx 8$ meV [30, 33]. The couplings J_1' and J_2' indicated by the thin dashed lines are roughly 10% of the dominant couplings. The first-neighbor coupling J_1'' on links between Te and W ions, the gray dashed line in (c), is about 4% of J_1 [33].

* sandvik@bu.edu
† slli@iphy.ac.cn

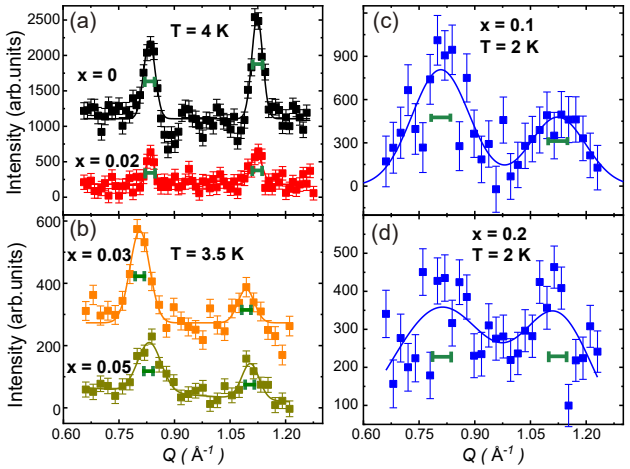

Figure 2. Neutron diffraction results for (a) x = 0 and 0.02, (b) 0.03 and 0.05 (c) 0.1, and (d) 0.2. The peaks correspond to wave-vectors q = (1/2,1/2,0) and (1/2,1/2,1) in the tetragonal magnetic Brillouin zone, indicating dominant Néel AFM order (x = 0 and 0.02) and short-range correlations ($x \geq 0.03$). Data at T = 40 K have been subtracted as background. The x = 0 and 0.03 values have been shifted vertically for clearity. The curves are Gaussian fits and the green bars indicate the instrumental resolutions.

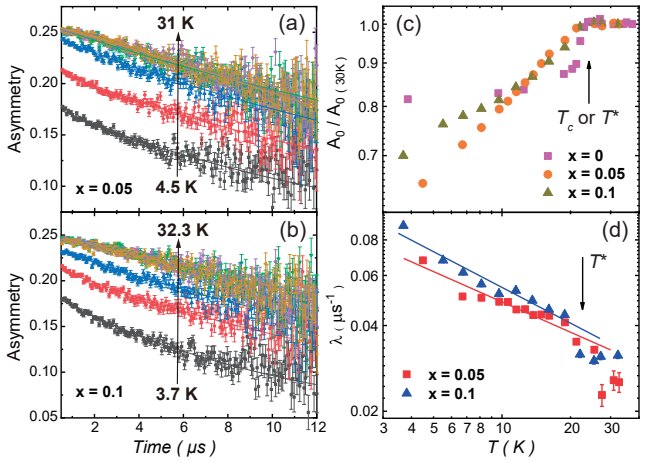

Figure 3. Time-dependent zero-field μSR spectra for (a) x = 0.05 and (b) $x = 0.1$ samples at different temperatures (the highest and lowest indicated) along with fits to Eq. (1). (c) Temperature dependent μSR asymmetry for x = 0, 0.05, and 0.1, normalized by the values at T = 30 K. (d) Temperature dependent relaxation rate λ for x = 0.05 and 0.1. The fitted lines correspond to critical scaling, $\lambda \approx T^{-\gamma}$, with γ = 0.35 $\pm$ 0.03 (x = 0.05) and 0.42 $\pm$ 0.03 (x = 0.1).

ions. Here 2D Néel order at temperature $T = 0$ is destroyed even at infinitesimal x, due to a logarithmic singularity caused by the single-impurity deformation of the spin texture. Order at $x > 0$ and $T > 0$ is stabilized by weak inter-layer couplings. The columnar AFM state extending from $x = 1$ is much more robust, which also can be explained by the classical model. In the non-magnetic phase, the neutron diffraction measurements reveal short-range Néel correlations and the μSR relaxation rate exhibits quantum-critical scaling with dynamic exponent $z > 2$, both consistent with recent predictions for the 2D RS state [22, 23].

Experiments.—Polycrystalline $Sr_2CuTe_{1-x}W_xO_6$ samples were synthesized as described previously [25–27, 29]. The experiments were carried out at J-PARC (μSR) and China Advanced Research Reactor and Key Laboratory of Neutron Physics and Institute of Nuclear Physics and Chemistry, China (neutron diffraction); see also Supplemental Material [34].

Figure 2 shows our neutron diffraction results. Resolution limited magnetic peaks are observed at x = 0 in Fig. 2(a), consistent with Néel AFM order [25, 30]. We have also confirmed (Supplemental Material [34]) columnar AFM order [31, 32] for $x \in [0.7, 1]$. The W doped sample with x = 0.02, Fig. 2(a), is still ordered, with resolution limited peaks (corresponding to a correlation length > 180 Å ≈ 35 lattice spacings). The broader peaks for $x \geq 0.03$ in Figs. 2(b)-2(d) indicate the loss of long-range order between x = 0.02 and 0.03. At x = 0.1 the correlation length is still about 40 Å.

The μSR asymmetry $A(t)$ was fitted to

$$A(t) = A_0 \exp(-\lambda t) G_z(t) + A_{\rm BG}, \qquad (1)$$

where A_0 is the initial asymmetry, λ the relaxation rate of the muon spins, $A_{\rm BG}$ the constant background, and $G_z(t)$ the Kubo-Toyabe function [35]. The function $A(t)$ cannot actually describe the complete muon spectra of the magnetically ordered samples. It has already been shown that, for columnar AFM ordered systems at x = 1, 0.9, and 0.8, the asymmetry initially drops very rapidly and oscillates [28, 32]. These features take place within 1 μs, beyond the resolution of our measurements. Instead, Eq. (1) describes the relaxation at longer times and A_0 is close to the asymmetry after the rapid initial drop. While the fits of Eq. (1) are not perfect for the long-range ordered samples (Supplemental Material [34]), the form describes the data for x = 0.05 and 0.1 very well, as shown in Figs. 3(a) and 3(b).

The temperature dependent A_0 is graphed in Fig. 3(c) for x = 0, 0.05 and 0.1. A sharp change is observed at the previously known ordering temperature T_c at x = 0 [25, 26]. In contrast, in the x = 0.05 and 0.1 samples A_0 only decreases slowly below a characteristic temperature T^*. This behavior reflects gradual changes of the local fields as a result of the onset of short-range magnetic correlations but no ordering, which is consistent with the neutron results in Figs. 2(b) and 2(c). It should be noted that the value of A_0 for x = 0 at low temperatures is about 4/5 of that above T_c, while in the case of x = 1 it is only 1/3 [27, 34]. It is beyond the scope of this work to explain the detailed form of A_0; some additional analysis is provided in Supplementary Material [34].

Fig. 3(d) shows the temperature dependence of the relaxation rate λ for x = 0.05 and 0.1. Power-law behaviors reflect quantum-critical scaling in what is likely the RS phase. As explained in Supplemental Material, standard scaling arguments [36, 37] in combination with a constraint imposed by the recently discovered $1/r^2$ form of the spin correlations in the 2D RS phase [22–24] can be used to derive the form $\lambda \propto T^{-\gamma}$ with $\gamma = 1 - 2/z$, where z is the dynamic exponent. The values of γ extracted from the fits in Fig. 3(d) correspond to

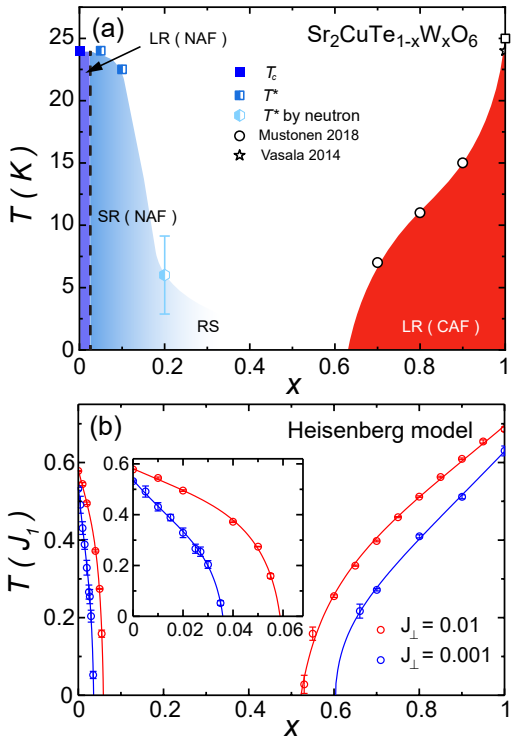

Figure 4. (a) Magnetic phase diagram of $Sr_2CuTe_{1-x}W_xO_6$. NAF and CAF denote Néel and columnar AFM correlations, respectively, either short-range (SR) or long-range (LR). The ordering temperature T_c and characteristic short-range correlation temperature T^* were determined by μSR measurements, except for T^* of the $x = 0.2$ sample, which was obtained (Supplemental Material [34]) by neutron diffraction (b) Transition temperatures of the classical Heisenberg model of coupled layers, determined using Monte Carlo simulations. In the notation of Fig. 1 the 2D couplings are $J_1 = J_2 = 1$, $J_1' = J_2' = 0.1$, and $J_1'' = 0$. Two different interlayer couplings are considered; $J_\perp = 10^{-2}$ and 10^{-3}. The curves drawn through the data points are only guides to the eye.

$z = 3.0 \pm 0.2$ for $x = 0.05$ and $z = 3.5 \pm 0.3$ for $x = 0.1$. These values conform with the expectations in the RS phase, where z equals 2 at the Néel–RS transition and grows upon moving into the RS phase [22]. It should be noted that the value of $A_{\rm BG}$ in Eq. (1) somewhat affects the determination of γ but we consistently find power law behavior of λ and $z(x = 0.1) > z(x = 0.05)$ (further discussed in Supplemental Material [34]). We note that the low-temperature μSR relaxation in quasi-2D spin glasses is very different [38].

Combining our μSR and neutron results with previous works, the magnetic phase diagram of $Sr_2CuTe_{1-x}W_xO_6$ is shown in Fig. 4(a). The columnar order at $x = 1$ is robust even for large Te substitution, which is indicative of only minor effects of magnetic frustration and remaining large connected ordered regions. The mean order parameter may then be gradually reduced in a way similar to diluted systems [39]. In contrast, introducing W in the $x = 0$ sample rapidly destroys the Néel order at $x_{c1} = 0.025 \pm 0.005$. Short-range correlations with Néel structure still remain at low temperatures even at $x = 0.2$ based on our neutron-diffraction experiments and likely persist throughout what we argue is the 2D RS phase.

Modeling.—The width of the Néel phase in Fig. 4(a) is less than $1/3$ of the previous estimates [30–32]. The Néel phase at finite W doping being narrower than the columnar phase at finite Te doping can be understood already at the classical level with the dominant Heisenberg coupling constants J_1 and J_2 in Fig. 1: Introducing a single Te impurity in the J_2-coupled columnar system, we simply lose the J_2 couplings in the affected plaquette and there is only weak frustration from the much smaller J_1' and J_1'' couplings. However, with a W impurity in the J_1-dominated Néel state the two new J_2 bonds are completely frustrated. To quantitatively understand the extremely narrow Néel phase requires further insights.

Ideally, we would like to carry out calculations with the full quantum mechanical Heisenberg Hamiltonian. Even though progress has been made on some frustrated 2D quantum magnets with density-matrix renormalization group (DMRG) [40] and tensor-product [41] methods, including Heisenberg systems with random couplings [24], in practice calculations for frustrated systems are still challenging and it would be hard to extract a reliable phase diagram. However, we have found that already the classical Heisenberg model can explain the extreme fragility of the Néel state to W-plaquette impurities and also give an overall reasonable phase diagram.

The long-range Néel order at $T = 0$ in the 2D Heisenberg model with uniform exchange $J_1 \mathbf{S}_i \cdot \mathbf{S}_j$ on all first neighbors (i, j) is destroyed by thermal fluctuations at $T > 0$ [42, 43]. In weakly coupled planes of classical or quantum spins, $T_c \propto J_1 \ln^{-1}(J_1/J_\perp)$, where $J_\perp$ is the coupling between spins in adjacent planes [44, 45]. Since a quantum magnet with AFM order or a long correlation length behaves in many respects as a "renormalized classical" system [43], the initial effects of doping the $x = 0$ and $x = 1$ system should be captured correctly by a classical model, up to $O(1)$ factors.

In the notation of Fig. 1, we set the 2D couplings to $J_1 = J_2 = 1$, $J_1' = J_2' = 0.1$, and $J_1'' = 0$, with $|\mathbf{S}_i| = 1$. For coupled planes we consider $J_\perp = 10^{-2}$ and 10^{-3}. We used standard Monte Carlo methods for frustrated Heisenberg models [46, 47], with Binder cumulant techniques [48] for extracting T_c at fixed x, based on averages over several hundred realizations of the random W and Te plaquettes on systems with up to $72 \times 72 \times 18$ spins. The resulting infinite-size extrapolated phase boundaries are shown in Fig. 4(b). When comparing with the experiments, it should be noted that $T = 25$ K corresponds roughly to 0.3 in units of J_1 and that T_c in uniform coupled $S = 1/2$ planes with $J_\perp$ of order 10^{-2} is lower by about 50% than our classical result at $x = 0$ [45]. We expect quantum fluctuations to shrink the ordered phases also in the x direction, and the differences between the numerical and experimental results for the columnar phase boundary should also be due to quantum effects (and possibly weak interactions beyond those included here).

As seen in Fig. 4(b), upon changing $J_\perp$ from 10^{-2} to 10^{-3}, T_c at $x = 0$ is only slightly reduced, as expected on account of the logarithmic form discussed above. For $x > 0$ the phase boundary drops more rapidly to zero for the smaller $J_\perp$, and the size of the Néel phase is substantially smaller. A very

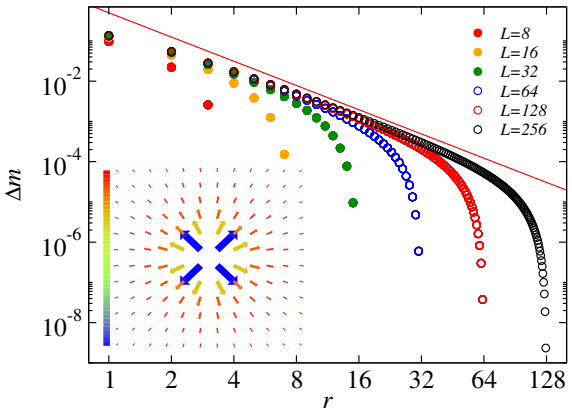

Figure 5. Deformation of the order parameter of the classical Heisenberg model with a W-type plaquette impurity as defined in Fig. 1, with the same couplings as in Fig. 4. The deviation $\Delta m = 1 - |S_i^z|$, where the z direction is that of the bulk Néel order, is shown vs the distance r from the impurity along the $(1, 0)$ lattice direction for several system sizes. The line shows the form $1/r^2$. The inset shows the projection of the spins to the xy spin plane, with the color coding corresponding to $m \in [0.49, 1]$. The magnitude of the xy component decays as $1/r$ from its maximal value ≈ 0.87 closest to the impurity. The behaviors correspond to an angular distortion $\propto 1/r$.

narrow Néel phase with high sensitivity of the $T = 0$ transition point to $J_\perp$ is not expected within a simple picture of conventional local impurity suppression of the order [39]. We therefore investigate the deformation of the Néel order around a single impurity plaquette at $T = 0$, which we have done by minimizing the energy with a combination of simulated annealing and energy conserving spin moves.

The deviation Δm of the local ordered moment from the bulk value is graphed in Fig. 5 versus the distance r from the impurity. The form $\Delta m \propto 1/r^2$ causes a logarithmic divergence when integrated over r (but the total energy cost of the deformation stays constant, with the energy density decaying as $1/r^4$). This single-impurity response suggests that any impurity fraction $x > 0$ destroys the long-range order, and this is demonstrated explicitly in the Supplemental Material [34]. A similar fragility of non-colinear bulk order in the presence of certain impurities was previously pointed out [8], but the profound impact of the plaquette impurity (which can be understood as a composite of two dipoles; see Supplemental Material [34]) on the colinear Néel state had not been anticipated.

For the weakly coupled planes in Fig. 4(b), the Néel order is stabilized for a range of $x > 0$ depending on $J_\perp/J_1$, but we have not studied the functional form of x_{c1} versus $J_\perp$. The disorder should be irrelevant at the $T > 0$ phase transitions according to the Harris criterion [49, 50], and we expect standard three-dimensional O(3) universality. We do not have sufficient data for large systems to test the critical exponents. In an $S = 1/2$ system such as $Sr_2CuTe_{1-x}W_xO_6$, quantum fluctuations should further suppress the order and reduce x_{c1}, and we expect the same type of logarithmic singularity as in the classical case when $J_\perp/J_1 \to 0$, on account of the renormalized classical picture of the quantum Néel state [43].

Discussion.—The extreme effect of the W impurities in the Néel state was not captured by the density functional calculations in Ref. [32], which suggested destabilization of the Néel order for $x \approx 0.1$-0.2 in $Sr_2CuTe_{1-x}W_xO_6$, significantly above $x_{c1} \approx 0.025$ found in our experiments. The mechanism we have uncovered here relies on a singular effect of frustrated plaquette impurities in 2D, with weak 3D couplings pushing the transition from $x = 0$ to to small $x > 0$.

Once the Néel order vanishes, from the classical perspective a spin glass phase is expected [8, 51]. In the presence of strong quantum fluctuations in $S = 1/2$ systems, there is mounting evidence from model studies that the spin glass can be supplanted by an RS state [8, 19, 22–24]. A particular realization of the RS state amenable to large-scale quantum Monte Carlo calculations exhibits criticality with a dynamic exponent $z \geq 2$ and dominant Néel-type spin correlations decaying with distance as $1/r^2$ at $T = 0$ [22, 23]. This form of the correlations was recently confirmed in a frustrated random-bond system with DMRG calculations [24], thus further supporting universal RS behavior. The significant staggered correlations well past the Néel phase in $Sr_2CuTe_{1-x}W_xO_6$, as revealed by our neutron difraction experiments at $x = 0.1$ and 0.2, are thus expected within the RS scenario. Previous results at $x = 0.5$ also showed remnants of Néel correlations [33]. We here further demonstrated quantum-critical scaling of the μSR relaxation rate with varying $z > 2$, as recently predicted in the 2D RS state [22, 23].

It would be interesting to further test the proposed RS scaling forms experimentally in $Sr_2CuTe_{1-x}W_xO_6$. A re-analysis [22] of susceptibility data for $x \geq 0.2$ [31] supported the predicted form $\chi \propto T^{-\gamma}$ with $\gamma < 1$. Detailed inelastic netron scattering studies would be very useful, but our attemps to grow large single-crystals have so far not been successful. With polycrystalline samples, NMR experiments may be able to further elucidate the nature of the RS state and the Néel–RS transition. RS signatures were previously reported in $YbMgGaO_4$ [20] and α-$Ru_{1-x}Ir_xCl_3$ [52], but in addition to random frustration these materials have Dzyaloshinskii-Moriya interactions and spin vacancies, respectively. Beyond its intrinsic importance, the 2D RS state should also be a useful benchmark for experiments on potential uniform spin liquids [53, 54], where it is often difficult [11, 20, 55, 56] to distinguish between impurity physics and theoretically predicted properties of clean systems.

ACKNOWLEDGMENTS

Acknowledgments.—W.H. and L.L contributed equally to this work. We would like to thank Oleg Sushkov for valuable comments. The research at Chinese institutions is supported by the National Key R&D Program of China (Grants No. 2017YFA0302900, No. 2016YFA0300502, No. 2018YFA0704201, No. 2016YFA0300604, No. 2017YFA0303100), the National Natural Science Foundation of China (Grants No. 11734002, No. 11775021, No. 11874401, No. 11874401, No. 11674406, No. 11822411, No. 12061130200, No. 11227906), and by the Strategic Priority Research Program (B) of the Chinese Academy of

Sciences (Grants No. XDB25000000 and No. XDB07020000, No. XDB28000000). H.L. is grateful for support from the Youth Innovation Promotion Association of CAS (Grant No. 2016004) and Beijing Natural Science Foundation (Grant No. JQ19002). The work in Boston was supported by the NSF under Grant No. DMR-1710170 and by the Simons Foundation under Simons Investigator Award No. 511064. L.L. would like to thank Boston University's Condensed Matter Theory Visitors Program for support. We also acknowledge the Super Computing Center of Beijing Normal University and Boston University's Research Computing Services for their support.

[1] P. A. Lee, N. Nagaosa, and X.-G. Wen, Doping a Mott insulator: Physics of high-temperature superconductivity, Rev. Mod. Phys. **78**, 17 (2006).

[2] S. Chatterjee, S. Sachdev, and M. S. Scheurer, Intertwining Topological Order and Broken Symmetry in a Theory of Fluctuating Spin-Density Waves, Phys. Rev. Lett. **119**, 227002 (2017).

[3] O. P. Vajk, P. K. Mang, M. Greven, P. M. Gehring, and J. W. Lynn, Quantum impurities in the two-dimensional spin one-half Heisenberg antiferromagnet, Science **295**, 1691 (2002).

[4] A. W. Sandvik, Classical percolation transition in the diluted two-dimensional S=1/2 Heisenberg antiferromagnet, Phys. Rev. B 66, 024418 (2002).

[5] C.-W. Liu, S. Liu, Y.-J. Kao, A. L. Chernyshev, and A. W. Sandvik, Impurity-Induced Frustration in Correlated Oxides, Phys. Rev. Lett. **102**, 167201 (2009).

[6] J. Ye, S. Sachdev, and N. Read, Solvable spin glass of quantum rotors, Phys. Rev. Lett. **70**, 4011 (1993).

[7] J. Oitmaa and O.P. Sushkov, Two-Dimensional Randomly Frustrated Spin-1/2 Heisenberg Model, Phys. Rev. Lett. **87**, 167206 (2001).

[8] S. Dey, E. C. Andrade, and M. Vojta, Destruction of long-range order in noncollinear two-dimensional antiferromagnets by random-bond disorder, Phys. Rev. B **101**, 020411(R) (2020).

[9] S. Sachdev and J. Ye, Gapless spin-fluid ground state in a random quantum Heisenberg magnet, Phys. Rev. Lett. **70**, 3339 (1993).

[10] M. Tarzia, G. Biroli, The Valence Bond Glass phase, Europhys. Lett. **82**, 67008 (2008).

[11] R. R. P. Singh, Valence Bond Glass Phase in Dilute Kagome Antiferromagnets, Phys. Rev. Lett. **104**, 177203 (2010).

[12] R. N. Bhatt and P. A. Lee, Scaling Studies of Highly Disordered Spin-1/2 Antiferromagnetic Systems, Phys. Rev. Lett. **48**, 344 (1982).

[13] D. S. Fisher, Random antiferromagnetic quantum spin chains, Phys. Rev. B **50**, 3799 (1994).

[14] O. Motrunich, S.-C. Mau, D. A. Huse, and D. S. Fisher, Infinite-Randomness Quantum Ising Critical Fixed Points, Phys. Rev. B **61**, 1160 (2000).

[15] Y.-C. Lin, R. Mélin, H. Rieger, and F. Iglói, Low-Energy Fixed Points of Random Heisenberg Models, Phys. Rev. B **68**, 024424 (2003).

[16] C. R. Laumman, D. A. Huse, A. W. W. Ludwing, G. Refael, S. Trebst, and M. Troyer, Strong-disorder renormalization for interacting non-Abelian anyon systems in two dimensions, Phys. Rev. B **85**, 224201 (2012).

[17] K. Watanabe, H. Kawamura, H. Nakano, and T. Sakai, Quantum Spin-Liquid Behavior in the Spin-1/2 Random Heisenberg Antiferromagnet on the Triangular Lattice, J. Phys. Soc. Jpn. **83** 034714 (2014).

[18] K. Uematsu, H. Kawamura, Randomness-induced quantum spin liquid behavior in the $s = \frac{1}{2}$ random J_1-J_2 Heisenberg antiferromagnet on the square lattice, Phys. Rev. B, **98**, 134427 (2018).

[19] I. Kimchi, A. Nahum, and T. Senthil, Valence Bonds in Random Quantum Magnets: Theory and Application to $YbMgGaO_4$, Phys. Rev. X **8**, 031028 (2018).

[20] I. Kimchi, J. P. Sheckelton, T. M. McQueen, and P. A. Lee, Scaling and data collapse from local moments in frustrated disordered quantum spin systems, Nat. Comm. **9**, 4367 (2018).

[21] H. Kawamura and K. Uematsu, Nature of the randomness-induced quantum spin liquids in two dimensions, J. Phys. Condens. Matter **31**, 504003 (2019),

[22] L. Liu, H. Shao, Y.-C. Lin, W. Guo, and A. W. Sandvik, Random-Singlet Phase in Disordered Two-Dimensional Quantum Magnets, Phys. Rev. X **8**, 041040 (2018).

[23] L. Liu, W. Guo, and A. W. Sandvik, Quantum-critical scaling properties of the two-dimensional random-singlet state, Phys. Rev. B **102**, 054443 (2020).

[24] H.-D. Ren, T.-Y. Xiong, H.-Q. Wu, D. N. Sheng, and S.-S. Gong, Characterizing random-singlet state in two-dimensional frustrated quantum magnets and implications for the double perovskite $Sr_2CuTe_{1-x}W_xO_6$, arXiv:2004.02128.

[25] T. Koga, N. Kurita, M. Avdeev, S. Danilkin, T. J. Sato, and H. Tanaka, Magnetic structure of the $S = \frac{1}{2}$ quasi-two-dimensional square-lattice Heisenberg antiferromagnet Sr_2CuTeO_6, Phys. Rev. B **93**, 054426 (2016).

[26] P. Babkevich, V. M. Katukuri, B. Fåk, S. Rols, T. Fennell, D. Pajić, H. Tanaka, T. Pardini, R. R. P. Singh, A. Mitrushchenkov, O. V. Yazyev, and H. M. Rønnow, Magnetic Excitations and Electronic Interactions in Sr_2CuTeO_6: A Spin-$1/2$ Square Lattice Heisenberg Antiferromagnet, Phys. Rev. Lett. **117**, 237203 (2016).

[27] S. Vasala, M. Avdeev, S. Danilkin, O. Chmaissem, and M Karppinen, Magnetic structure of Sr_2CuWO_6, J. Phys.: Condens. Matter **26**, 496001 (2014).

[28] S. Vasala, H. Saadaoui, E. Morenzoni, O. Chmaissem, T.S. Chan, J.-M. Chen, Y.-Y. Hsu, H. Yamauchi, and M. Karppinen, Characterization of magnetic properties of Sr_2CuWO_6 and Sr_2CuMoO_6, Phys. Rev. B, **89**, 134419 (2014).

[29] H. C. Walker, O. Mustonen, S. Vasala, D. J. Voneshen, M. D. Le, D. T. Adroja, and M. Karppinen, Spin wave excitations in the tetragonal double perovskite Sr_2CuWO_6, Phys. Rev. B **94**, 064411 (2016).

[30] O. Mustonen, S. Vasala, E. Sadrollahi, K. P. Schmidt, C. Baines, H. C. Walker, I. Terasaki, F. J. Litterst, E. Baggio-Saitovitch, and M. Karppinen, Spin-liquid-like state in a spin-1/2 square-lattice antiferromagnet perovskite induced by d^{10}-d^0 cation mixing, Nat. Commun. **9**, 1085 (2018).

[31] M. Watanabe, N. Kurita, H. d Tanaka, W. Ueno, K. Matsui, and T. Goto, Valence-bond-glass state with a singlet gap in the spin-$\frac{1}{2}$ square-lattice random J_1-J_2 Heisenberg antiferromagnet $Sr_2CuTe_{1-x}W_xO_6$, Phys. Rev. B **98**, 054422 (2018).

[32] O. Mustonen, S. Vasala, K. P. Schmidt, E. Sadrollahi, H. C. Walker, I. Terasaki, F. J. Litterst, E. Baggio-Saitovitch, M. and Karppinen, Tuning the $S = 1/2$ square-lattice antiferromagnet $Sr_2Cu(Te_{1-x}W_x)O_6$ from Néel order to quantum disorder to

columnar order, Phys. Rev. B, **98**, 064411 (2018).
[33] V. M. Katukuri, P. Babkevich, O. Mustonen, H. C. Walker, B. Fåk S. Vasala, M. Karppinen, H. M. Rønnow, and O. V. Yazyev, Exchange Interactions Mediated by Nonmagnetic Cations in Double Perovskites, Phys. Rev. Lett. **124**, 077202 (2020).
[34] See Supplemental Material for experimental details, quantum-critical scaling forms, and additional Monte Carlo results, which includes references 57-62.
[35] R. S. Hayano, Y. J. Uemura, J. Imazato, N. Nishida, T. Yamazaki, and R. Kubo, Zero-and low-field spin relaxation studied by positive muons, Phys. Rev. B **20**, 850 (1979).
[36] M. P. A. Fisher, P. B. Weichman, G. Grinstein, and D. S. Fisher, Boson localization and the superfluid-insulator transition, Phys. Rev. B **40**, 546 (1989).
[37] A. V. Chubukov and S. Sachdev, Universal Magnetic Properties of $La_{2-\delta}Sr_{\delta}CuO_4$ at Intermediate Temperatures, Phys. Rev. Lett. **71**, 169 (1993).
[38] P. Yadav, S. Sharma, P. J. Baker, P. K. Biswas, I. da Silva, R. Raghunathan, U. Deshpande, R. J. Choudhary, N. P. Lalla, and A. Banerjee, μSR and neutron diffraction studies on the tuning of spin-glass phases in the partially ordered double perovskites $SrMn_{1x}W_xO_3$, Phys. Rev. B **99**, 214421 (2019).
[39] M. F. Collins, *Magnetic Critical Scattering* (Oxford University Press, New York 1989).
[40] R. Verresen, F. Pollmann, and R. Moessner, Quantum dynamics of the square-lattice Heisenberg model, Phys. Rev. B **98**, 155102 (2018).
[41] L. Chen, D.-W. Qu, H. Li, B.-B. Chen, S.-S. Gong, J. von Delft, A. Weichselbaum, and W. Li, Two-temperature scales in the triangular-lattice Heisenberg antiferromagnet, Phys. Rev. B **99**, 140404(R) (2019).
[42] N. D. Mermin and H. Wagner, Absence of Ferromagnetism or Antiferromagnetism in One- or Two-Dimensional Isotropic Heisenberg Models, Phys. Rev. Lett. **17**, 1133 (1966).
[43] S. Chakravarty, B. I. Halperin, and D. R. Nelson, Two-dimensional quantum Heisenberg antiferromagnet at low temperatures, Phys. Rev. B **39**, 2344 (1989).
[44] V. Y. Irkhin and A. A. Katanin, Thermodynamics of isotropic and anisotropic layered magnets: renormalization-group approach and 1/N expansion. Phys. Rev. B **57**, 379 (1998).
[45] P. Sengupta, A. W. Sandvik, and R. R. P. Singh, Specific heat of quasi-two-dimensional antiferromagnetic Heisenberg models with varying interplanar couplings, Phys. Rev. B **68**, 094423 (2003).
[46] J. Alonso, A. A. tarancón, H. Ballestros, L. Fernándes, V. Martín-Mayor, A. Munõs Sudupe, Monte Carlo study of O(3) antiferromagnetic models in three dimensions, Phys. Rev. B **53**, 2537 (1996).
[47] L. W. Lee and A. P. Young, Large-scale Monte Carlo simulations of the isotropic three-dimensional Heisenberg spin glass, Phys. Rev. B **76**, 024405 (2007).
[48] A. W. Sandvik, Computational Studies of Quantum Spin Systems, AIP Conf. Proc. **1297**, 135 (2010).
[49] A. B. Harris, Effect of random defects on the critical behaviour of Ising models, J. Phys. C **7**, 1671 (1974).
[50] J. T. Chayes, L. Chayes, D. S. Fisher, and T. Spencer, Finite-size scaling and correlation lengths for disordered systems, Phys. Rev. Lett. **57**, 2999 (1986).
[51] Y. Xu and D.-X. Yao, Spin glass in the bond-diluted J_1-J_2 Ising model on the square lattice, Phys. Rev. B **97**, 224419 (2018).
[52] S.-H. Baek, H. W. Yeo, S.-H. Do, K.-Y. Choi, L. Janssen, M. Vojta and B. Büchner, Observation of a gapless spin liquid in a diluted Kitaev honeycomb material, Phys. Rev. B **102**, 094407 (2020).
[53] L. Savary and L. Balents, Quantum spin liquids: a review, Rep. Prog. Phys. **80**, 016502 (2017).
[54] Y. Zhou, K. Kanoda, and T.-K. Ng, Quantum spin liquid states, Rev. Mod. Phys. **89**, 025003 (2017).
[55] Y. Li, G. Chen, W. Tong, L. Pi, J. Liu, Z. Yang, X. Wang, and Q. Zhang, Rare-Earth Triangular Lattice Spin Liquid: A Single-Crystal Study of $YbMgGaO_4$, Phys. Rev. Lett. **115**, 167203 (2015).
[56] Z. Ma *et al.*, Spin-Glass Ground State in a Triangular-Lattice Compound $YbZnGaO_4$, Phys. Rev. Lett. **120**, 087201 (2018).
[57] C. Slichter, *Principles of Magnetic Resonance*, 3rd ed. (Springer-Verlag, Berlin, Heidelberg, 1990).
[58] Y.-R. Shu, M. Dupont, D.-X. Yao, S. Capponi, and A. W. Sandvik, Dynamical properties of the S = 1/2 random Heisenberg chain, Phys. Rev. B **97**, 104424 (2018).
[59] M. Randeria, N. Trivedi, A. Moreo, and R. T. Scalettar, Pairing and spin gap in the normal state of short coherence length superconductors, Phys. Rev. Lett. **69**, 2001 (1992).
[60] O. P. Sushkov, Long-range dynamics related to magnetic impurities in the two-dimensional Heisenberg antiferromagnet, Phys. Rev. B **68**, 094426 (2003).
[61] L. Lu, W. Guo, and A. W. Sandvik (in preparation).
[62] J. Vannimenus, S. Kirkpatrick, F. D. M. Haldane, C. Jayaprakash, Ground-state morphology of random frustrated XY systems, Phys. Rev. B **39** 4634 (1989).